International Journal of Applied Earth Observations and Geoinformation 103 (2021) 102514

Contents lists available at ScienceDirect

International Journal of Applied Earth Observations and Geoinformation

journal homepage: www.elsevier.com/locate/jag

Integrating remote sensing and geospatial big data for urban land use mapping: A review

Jiadi Yin[a,b], Jinwei Dong[a,*], Nicholas A.S. Hamm[b], Zhichao Li[a], Jianghao Wang[c], Hanfa Xing[d,e], Ping Fu[b]

[a] Key Laboratory of Land Surface Pattern and Simulation, Institute of Geographic Sciences and Natural Resources Research, Chinese Academy of Sciences, Beijing 100101, China
[b] School of Geographical Sciences and Geospatial Research Group, Faculty of Science and Engineering, University of Nottingham, Ningbo 315100, China
[c] State Key Laboratory of Resources and Environmental Information System, Institute of Geographic Sciences and Natural Resources Research, Chinese Academy of Sciences, Beijing 100101, China
[d] College of Geography and Environment, Shandong Normal University, Jinan 250300, China
[e] School of Geography, South China Normal University, Guangzhou 510631, China

ARTICLE INFO

Keywords:
Integration methods
Urban functional zone classification
Urban management
Land use

ABSTRACT

Remote Sensing (RS) has been used in urban mapping for a long time; however, the complexity and diversity of urban functional patterns are difficult to be captured by RS only. Emerging Geospatial Big Data (GBD) are considered as the supplement to RS data, and help to contribute to our understanding of urban lands from physical aspects (i.e., urban land cover) to socioeconomic aspects (i.e., urban land use). Integrating RS and GBD could be an effective way to combine physical and socioeconomic aspects with great potential for high-quality urban land use classification. In this study, we reviewed the existing literature and focused on the state-of-the-art and perspective of the urban land use categorization by integrating RS and GBD. Specifically, the commonly used RS features (e.g., spectral, textural, temporal, and spatial features) and GBD features (e.g., spatial, temporal, semantic, and sequence features) were identified and analyzed in urban land use classification. The integration strategies for RS and GBD features were categorized into feature-level integration (FI) and decision-level integration (DI). To be more specific, the FI method integrates the RS and GBD features and classifies urban land use types using the integrated feature sets; the DI method processes RS and GBD independently and then merges the classification results based on decision rules. We also discussed other critical issues, including analysis unit setting, parcel segmentation, parcel labeling of land use types, and data integration. Our findings provide a retrospect of different features from RS and GBD, strategies of RS and GBD integration, and their pros and cons, which could help to define the framework for future urban land use mapping and better support urban planning, urban environment assessment, urban disaster monitoring and urban traffic analysis.

1. Introduction

With the advent of the Anthropocene (Ellis and Ramankutty, 2008; Steffen et al., 2011), urbanization is accelerating and the urban population is predicted to grow from 4.2 billion (57.5% of the world population) in 2018 to about 6.7 billion (69.1%) in 2050 (Seto et al., 2011). Such increasing human-induced influences are changing urban land in different dimensions from physical aspects (urban land cover) to socioeconomic aspects (urban land use) (Elmqvist et al., 2019; Hersperger et al., 2018). A large number of high-accuracy urban land cover products (mainly physical characteristics) at the annual level with relatively high spatial resolution have been developed worldwide (Li et al., 2020a; Liu et al., 2018; Zhou et al., 2018). However, urban land governance and planning need more information on urban land use, which is particularly complex and includes both physical aspects and socioeconomic aspects. Unfortunately, high-quality urban land use products with timely and accurate information related to human activities are still limited (Gong et al., 2020). Understanding the start-of-the-art of existing urban land use mapping efforts, considering both physical and socioeconomic functions, would enable better urban land management and monitoring (Martí et al., 2019; Yammine et al., 2018).

A wide range of satellite remote sensing (RS) data (e.g., Moderate-

* Corresponding author.
E-mail address: dongjw@igsnrr.ac.cn (J. Dong).

https://doi.org/10.1016/j.jag.2021.102514
Received 2 June 2021; Received in revised form 8 August 2021; Accepted 20 August 2021

resolution Imaging Spectroradiometer (MODIS), Landsat TM/ETM/OLS, Defense Meteorological Satellite Program Operation Linescan System (DMSP-OLS)) have been used to study the structures, boundaries, and areas of cities (Huang et al., 2021; Gong et al., 2019a; Schneider et al., 2010). Nevertheless, the complexity and diversity of functional patterns in urban areas cannot be captured well by using RS only due to limited information (e.g. spectral, textural, and temporal information) from RS techniques (Cao et al., 2020). Advances in information and communication technologies make it possible to get access to geospatial big data (GBD) (Li et al., 2016; Li et al., 2021; Yin et al., 2021). Fixed and mobile sensors such as environmental sensors, cameras, webcams, social media, or even urban residents through their regular activities (Wu et al., 2015) create tremendous GBD every day. These data such as mobile phone data (Gong et al., 2020), traffic trajectories (Yu et al., 2019), geo-tagged photos (Cadavid Restrepo et al., 2017; Krylov et al., 2018), Points of interest (POIs) (Yin et al., 2021) and social media data (Huang et al., 2018) provide an alternative approach to uncover how cities function (Ye et al., 2016). It is possible for examining the physical and socioeconomic characteristics of the urban land system by taking both the advantages of RS and GBD (Qi et al., 2019; Song et al., 2021; Zhang et al., 2021a; Xiong et al., 2021; Zhang et al., 2021b).

Despite the great potential of integrating RS and GBD for providing better insights into urban land use, it is challenging to combine them due to the differences in the spatial data quality (e.g., semantic, timestamp, and scale), technical format, and data structure (Liu et al., 2015). Summarizing the features of RS and GBD and integration strategies in the literature are needed for guiding future studies and help to understand more detailed urban functional patterns.

In this context, this study examined the literature on the nature of RS and GBD, as well as their integration strategies in urban land use classification, and identified the opportunities and challenges for synthesizing RS and GBD (Table S1). The primary objective of this paper is to review the state-of-the-art in this field by considering (1) the key characteristics of RS and GBD and (2) the methods for integrating RS and GBD. We consider only satellite-based RS and do not consider RS data obtained from airborne platforms. This review is organized into six sections. Section 2 summarized the transformation from urban land cover to urban land use. In section 3, we summarized the commonly used RS and GBD features for urban land use categorization. In Section 4, the integration strategies were analyzed systematically. In Section 5, we discussed the challenges and potential applications of the integration of RS and GBD on urban land use maps. Section 6 concluded the main findings and implications.

2. Evolution from urban land cover to urban land use

Using satellite data to map urban land cover has a long history (Howarth and Boasson, 1983; Patino and Duque, 2013; Reba and Seto, 2020). Examples of existing efforts for global urban land cover products that have been derived from RS are shown in Table 1. The data source, the nomenclature of urban land, spatial resolution, time period, and reference for each global urban land cover map were summarized. Most urban land cover maps were obtained from coarse spatial resolution images (100 m-10 km), such as MODIS and Advanced Very High-Resolution Radiometer (AVHRR) (Friedl et al., 2002; Schneider et al., 2010). With the substantial progress of RS techniques, recent maps were derived from moderate spatial resolution images (10–100 m), including Satellite Pour l' Observation de la Terre (SPOT) and Landsat images (Deng et al., 2019; Li et al., 2020a). The time period of these global urban land cover products has transformed from a single period to repeated observations, which could provide better quality and time series urban land cover information (Gong et al., 2019a; Li et al., 2020b). Overall, these global urban RS studies focused on the identification of physical urban attributes (e.g., impervious surface, built-up areas, artificial surfaces, and urban extent) that have provided opportunities for a better understanding of global urbanization's effects on human civilization and the environment (Zhu et al., 2019). Despite the aforementioned extensive applications of RS data for mapping urban land cover, more specific information of inner-urban functions cannot be retrieved by using RS only (Li et al., 2017a; Liu et al., 2015).

The demands for urban land products have changed gradually, with increasing information needs on socioeconomic properties, emphasizing a transformation from urban land cover to urban land use (Fig. 1). The multi-sourced GBD can contribute to the understanding of socioeconomic characteristics of urban land use, and identify how people use lands (Srivastava et al., 2018; Zhang et al., 2019a; Zhao et al., 2018). Recently, GBD has been used in conjunction with RS data to extract urban land use information (Liu et al., 2020a; Shi et al., 2019). Therefore, understanding characteristics derived from RS and GBD and their integration methods are necessary for urban land use mapping (Li et al., 2017a; Qi et al., 2019).

Table 1
Comparison of existing global urban land cover products.

Products	Data	Nomenclature of urban land	Spatial resolution	Time period	Reference
GLCC	AVHRR	Built-up areas	1 km	1992,1993	Loveland et al., 2000
UMD1km	AVHRR	Urban and built	1 km	1992,1993	Hansen et al., 2000
GRUMP	VMAP, Census data, DMSP-OLS, Maps	Urban extent	1 km	1995	CIESIN et al., 2011
GLC2000	SPOT-Vegetation, DMSP-OLS	Artificial surfaces and associated areas	1 km	2000	Bartholomé and Belward, 2005
IMPSA	DMSP-OLS	Impervious surface	1 km	2000	Elvidge et al., 2007
NTL-Urban	DMSP-OLS	Urban extent	1 km	1992–2013	Zhou et al., 2018
MOD500	MODIS	Non-vegetated, human-constructed elements	500 *m*	2001–2017	Friedl et al., 2002
GHSL	Fine-scale satellite imagery, census data, and OSM	Built-up areas	500 *m*	1975, 1990, 2000, 2015	Pesaresi et al., 2013
GlobCover	SPOT-Vegetation	Artificial surfaces and associated areas	300 *m*	2005, 2009	Arino et al., 2007
CCI-LC	SPOT-Vegetation	Urban extent	300 *m*	1992–2015	Defourny et al., 2018
GlobaLand30	Landsat TM/ETM+	Artificial surfaces	30 *m*	2000, 2010	Chen et al., 2015
HBASE	Landsat TM/ETM+	Built-up and settlement extent	30 *m*	2010	Wang et al., 2017
GMIS	Landsat TM/ETM+	Impervious surface	30 *m*	2010	Colstoun et al., 2017
FROM-GLC	Landsat TM/ETM+/OLI	Impervious surface	30 *m*	2010, 2015, 2017	Gong et al., 2013
Global Urban Land	Landsat TM/ETM+	Impervious surface	30 *m*	1990, 1995, 2000, 2005, 2010	Liu et al., 2018
GUF	TerraSAR-X, TanDEM-X	Built-up areas	12 *m*	2011	Esch et al., 2012
FROM-GLC10	Sentinel	Impervious surface	10 *m*	2017	Gong et al., 2019b

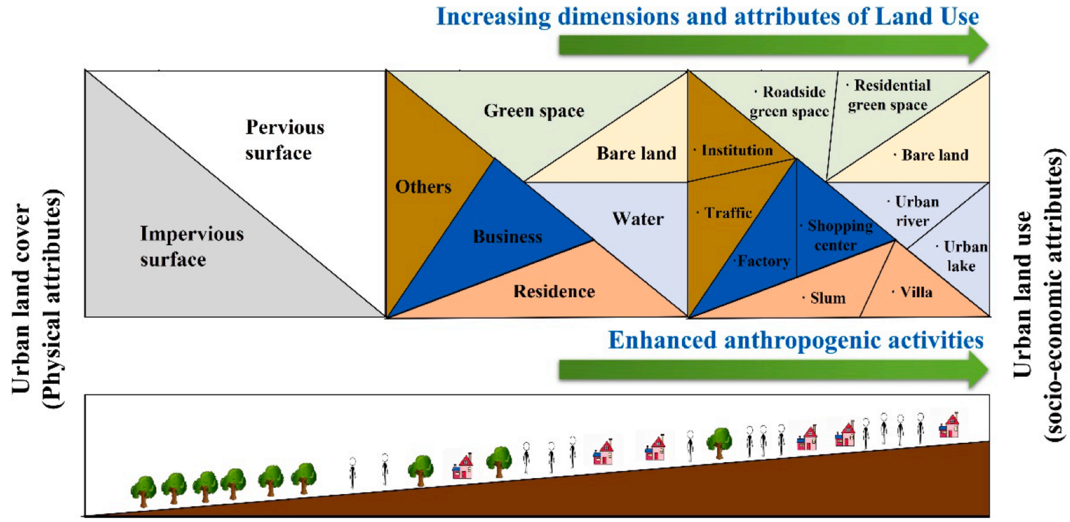

Fig. 1. Transformation of the need for urban land products from physical attributes to socioeconomic attributes due to enhanced anthropogenic activities. The three boxes above represent the transformation from urban land cover (e.g., impervious surface and pervious surface) to urban land use (e.g., traffic, institution, urban lake, residential green space, and others). The box below refers to the enhanced human impacts on urban areas. It should be noted that the change of area proportions of different urban land use types is not reflected in Fig. 1. (For interpretation of the references to colour in this figure legend, the reader is referred to the web version of this article.)

3. RS and GBD features for urban land use mapping

The extraction of RS and GBD features is the most essential procedure for urban land use recognition because the performance of urban land use maps relies heavily on these features. The purpose of this section is thus to introduce several commonly used RS and GBD features

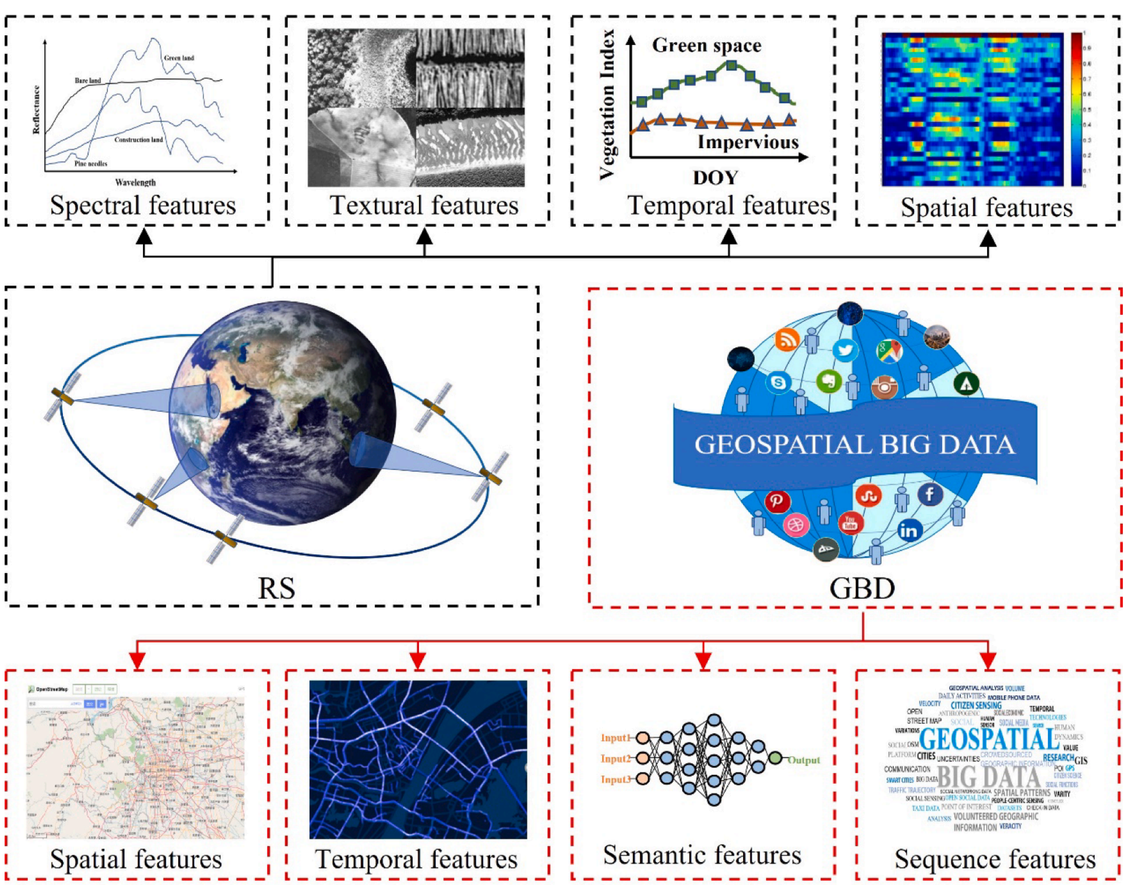

Fig. 2. Summary of the features of RS and GBD. The dotted black box and red box in the middle show the commonly used RS data (e.g., MODIS, Landsat, Sentinel) and GBD (e.g., traffic, social media data, geo-tagged photos), respectively. The upper dotted black boxes represent the features (spectral, textural, temporal, and spatial) extracted from RS, while the dotted red boxes below represent the features (spatial, temporal, semantic, and sequence) extracted from GBD. (For interpretation of the references to colour in this figure legend, the reader is referred to the web version of this article.)

for categorizing urban land use types (Fig. 2).

3.1. RS-based features

The features derived from RS images used in urban land use classification could be categorized into spectral, textural, temporal, and spatial features (Gong and Howarth, 1989; Zhu et al., 2017). Among them, spectral and textural features are common characteristics of RS data to extract urban land use information because different textures and spectra could reflect different urban land use types (Zhu et al., 2019). The temporal features have proven beneficial for improving urban land use maps by providing valuable information (e.g., time series information) on urban land use types (Zhu et al., 2012). Recently, deep learning techniques provide new possibilities for extracting spatial features automatically from the very-high-resolution (VHR) satellite imageries such as WorldView-3, Gaofen-2, and SPOT-5 (Zhang et al., 2020). Spatial features could help classify urban land use at a very detailed level (Zhao et al., 2019). The details of the RS features are specified as follows.

(1) Spectral features: Generally, the spectral features of urban land show lower reflectance in the near-infrared region (NIR), comparing to vegetation, which has higher reflectance in NIR (Herold et al., 2003). Additionally, the spectra for the visible, short-wave infrared region (SWIR) and microwave regions were also found to be suitable for characterizing urban objects (Heiden et al., 2007). Recently, spectral features from the increased number of bands (e.g., from Landsat to Sentinel-2) provide an opportunity for the acquisition of detailed information on the physical attributes of urban land use, but it also leads to data redundancy due to the high correlation between adjacent bands (Okujeni et al., 2018). Liu et al. (2020b) and Zhang et al. (2017b) extracted spectral features from RS imagery for classifying urban land use. Both the methods calculated the mean and standard deviation of each band by using a certain window.

(2) Textural features: Textural features contain rich information of the spatial distribution of tonal changes, as well as the structural arrangement of surfaces and their relationships to the surrounding environment (Gong and Howarth, 1989; Haralick et al., 1973). Different textures (e.g., coarse, smooth, rippled, irregular, and lineated) show different image characteristics, such as homogeneity, linear structure, and contrast (Kuffer et al., 2016; Wurm et al., 2017). Therefore, textural features could help to increase the accuracy of land use categorization in heterogeneous landscapes (Jin et al., 2014; Pacifici et al., 2009), where ground objects with different sizes, patterns, structures, and shapes coexist (Lu and Weng, 2006).

(3) Temporal features: Temporal features refer to the differences caused by the changes in the spectral and textural features of urban surfaces over time. Due to the seasonality of vegetation growth, it has proven to be effective in improving vegetation and other land cover mapping accuracy (Dong and Xiao, 2016; Zurita-Milla et al., 2013). The extraction of urban land usually tends to be less accurate in the autumn and winter due to more bare land (Weng et al., 2009). However, it is still a challenge to distinguish the variety of processes that generate different time series, for example, due to climate, topography, and terrestrial vegetation (Pflugmacher et al., 2019).

(4) Spatial features: Along with spectral, textural, and temporal features, the most commonly used feature extracted from RS data is the spatial feature. Recent studies used deep learning techniques such as the supervised convolutional neural network (CNN) models and unsupervised autoencoders (AE) models to extract spatial information automatically from RS images (Reichstein et al., 2019). Deep learning algorithms, which extract high-level spatial information provided by hierarchical structures, demonstrate remarkable capacity in image representation and understanding in these studies. Traditional approaches such as Random forest models (RF), Support vector machine (SVM), and Decision tree (DT) can only process basic features (e.g., spectral, textural, and temporal features) from RS images. Due to the fine structural information (i.e., spatial details) of urban land use in VHR RS images, VHR RS images were found to be commonly used by deep learning techniques for obtaining urban land use information (Ma et al., 2019).

3.2. GBD-based features

The development of mobile positioning, wireless communication, and the Internet of Things (IoT) provides opportunities for the rapid growth of big data (Kitchin, 2013). According to Kitchin and McArdle (2016), big data is defined in part by its large size and in part by its characteristics, such as volume, variety, and velocity. Liu et al. (2016) further defined the characteristics of big data as exhaustivity, relationality, veracity, value, and variability. In the IBM Annual Report, 2.5 terabytes of data are generated every day, with 80% of these data (pictures, texts, and videos) being geo-referenced or capable of being geo-referenced. Therefore, a large proportion of big data is likely to be the GBD (i.e., big data with geographical reference). GBD is generated every day mostly by fixed and mobile sensors such as environmental sensors, cameras, webcams, social media, or even residents' daily activities (Brovelli et al., 2015).

The most commonly used GBD for land use mapping are social sensing (SS) (Liu et al., 2015), citizen sensing (CS) (Jiang et al., 2016), social media data (SMD) (Ilieva and McPhearson, 2018), and volunteered geographic information(VGI) (Goodchild and Glennon, 2010). The descriptions of SS, CS, SMD, and VGI are provided in Table 2. The contents and concepts of SS and CS are much broader than GBD. SS data is used in a variety of applications besides urban land use mapping. CS does not contain the data produced by companies and institutions and VGI focuses on user-generated data. However, the term GBD encompasses all of these above-mentioned geospatial data.

Each record of GBD contains spatial, temporal, semantic, and/or sequence information associated with individuals reflecting human behavior, although the quality of this information may vary in space and time (Fig. 2 and Table 3). Due to the high correlation between human spatiotemporal activities and urban dynamic socioeconomic attributes, these emerging GBD can help to capture the growing complexity of urban functional patterns (Wu et al., 2018). Therefore, in order to better classify and understand urban land use, we add GBD to the identification of socioeconomic and human activities.

(1) Spatial features: Almost all GBD can provide spatial information (Table 3). For example, the OSM has proven to be a useful spatial

Table 2
Comparison of concepts related to GBD in previous studies.

Concepts	Refs.	Description
Social Sensing (SS)	Liu et al., 2015	A series of data sources with spatiotemporal information which record human activities, as well as the methods and applications based on such data source.
Citizen Sensing (CS)	Jiang et al., 2016	Datasets contributed by citizens provide benefits for themselves and policymakers.
Social Media Data (SMD)	Ilieva and McPhearson, 2018	Information of 'big data' from social media such as Facebook, Flickr, etc.
Volunteered Geographic Information (VGI)	Goodchild and Glennon, 2010	Geographic data provided voluntarily by people use technologies to generate, assemble, and disseminate information.

Table 3
Summary of the GBD and relevant features used in urban land use mapping.

Data sources	Spatial features	Temporal features	Semantic features	Sequence features
Mobile phone data	√	√		
Traffic data	√	√		
Social media data	√	√	√	√
Geo-tagged photos	√		√	
Maps	√			√
Search engine data	√		√	√
Smart card data	√	√		

data source including land use information like buildings, roads, and parks (Helbich et al., 2012), which could be used to extract training pixels from RS images for classifying urban land use types (Johnson and Iizuka, 2016; Wan et al., 2017). Google maps, Gaode maps, and other maps have also been successfully applied to urban land use mapping (Xu et al., 2020; Zhang et al., 2020). Furthermore, social media data can provide indirect spatial location data (Long et al., 2018; Yao et al., 2018), for example, Zhan et al. (2014) inferred the urban land use types in Now York city by using check-in social media data on Twitter.

(2) Temporal features: There are many examples of data sources (e.g., mobile phone data, traffic data, social media data, and smart card data) with temporal features that could reveal the mobility patterns of human activities (Pan et al., 2013; Wu et al., 2018). For instance, Gong et al. (2015) analyzed the spatiotemporal characteristics of nine daily activity types referring to the trip purposes of taxi trajectory data. Shi et al. (2019) extracted the temporal variation in WeChat (i.e., WeChat is China's most popular messaging app) user density from different land use categories for urban land use classification combined with RS data. The activities of human beings with temporal features can be determined to indicate the social function and patterns of urban land use (Chen et al., 2017; Frias-Martinez and Frias-Martinez, 2014; Pei et al., 2014).

(3) Semantic features: Photographs are an important element of GBD. Examples include street view photographs, crowd-sourced geo-tagged photos, and social media photos (Kang et al., 2018; Xu et al., 2017). Semantic features obtained from photographs have much in common with those obtained from RS data. However, there are also important distinctions that present challenges for analysis. RS is usually undertaken by national and international organizations following established scientific and engineering principles, including regular acquisition cycles (Ursula et al., 2004). While crowdsourced photographs may be acquired by a range of organizations (e.g., Google Street View) and private individuals. They provide fine-resolution data, but the spatial and temporal sampling may be ad hoc, and the quality can be highly variable (Hu et al., 2015). Recently, with the development of image recognition and deep learning technology, extracting semantic features from photographs and applying them to the perception of places have become possible (Xu et al., 2017).

(4) Sequence features: Social media data and search engine data have become an important source of GBD in current research (Zheng et al., 2019). Studies utilizing sequence features mainly include the following three aspects (Long and Liu, 2017): (a) to obtain the evaluation index or topic of a place; (b) to obtain information on emotions related to the place, such as happiness or depression (Yang and Mu, 2015; Zheng et al., 2019); (c) to identify public attention to hot events, such as disasters, diseases, and accidents. Specific examples of sequence information include sentiment, opinions, locations, time, and places. For example, Mitchell et al. (2013) generated a method for analyzing the correlations between human being's real-time expressions and others like emotional, geographic, and demographic characteristics.

4. Integration of RS and GBD for urban land use mapping

The RS and GBD features can be then combined using different approaches for urban land use categorization. According to the fusion mode between RS and GBD features, RS and GBD integration techniques in the literature could be divided into feature-level integration (FI) and decision-level integration (DI).

4.1. Feature-level integration

In FI-based classification, RS features (e.g., spectral, textural, temporal, and spatial features), and GBD features (e.g., spatial, temporal, semantic, sequence features) are first extracted. These features are fused into integrated feature sets for urban land use classification (Fig. 3).

Several efforts have been made for extracting urban land use information using the FI method (Bao et al., 2020; Chang et al., 2020; Hu et al., 2016; Zhang et al., 2017a). For the study unit of the FI-based classification, most studies utilized parcel-level or object-level as the study unit since object-level or parcel-level units are compatible with both RS features and GBD features (Liu et al., 2017). To be more specific, the format of the RS features is usually grid, while for the GBD features is various. It is thus necessary to unify the two kinds of features. Parcel-level classification units can be generated by using the OSM road network or other road data (Huang et al., 2020). The urban parcels are obtained by removing the road buffers from the study site. Sometimes, the study site should also exclude the rivers according to the actual situation. Furthermore, the elevated road in cities would interfere with the segmentation results and need to be considered. Pixel-based and grid-based units are also used for FI-based urban land use classification (Dong et al., 2020).

For the feature extraction stage, the FI-based classification method extracts RS and GBD features respectively. For example, Zhang et al. (2019b) delineated physical features including spectral features (e.g., mean and standard deviation for each band), textural features (e.g., contrast, entropy, correlation, and homogeneity for each band) from RS for urban land use categorization by integrating GBD features (e.g., POI words and real-time Tencent users words). Sun et al. (2020) extracted RS features (spectral and textural features), GBD features (POI frequency, POI spatial distribution), and other features to train the RF classifier for recognizing urban functions (e.g., residence, business, and industries).

In the feature integration stage, the FI method usually classifies RS and GBD features by using machine learning techniques such as RF classifier, SVM, and DT. For example, Gong et al. (2020) proposed a research method that is extracting several features from RS and GBD for training the RF classifier, which has proven to be a new way for mapping urban land use over large areas. Du et al. (2020) generated urban functional zones by removing road buffers, and then the functional zones were classified by coupling Latent Dirichlet Allocation (LDA) and SVM. The proposed method is promising for urban land use mapping over large areas. Recently, deep learning techniques such as CNN and AE models are also used for urban land use mapping, which could help improve the classification performance (Mao et al., 2020).

4.2. Decision-level integration

For categorizing urban land use, DI-based classification combines RS-based classification results with GBD-based classification results. To be more specific, RS and GBD features are evaluated independently before being integrated for urban land use mapping utilizing various modes and methods (Fig. 4).

Compared to the FI method, the basic unit for the DI method is more

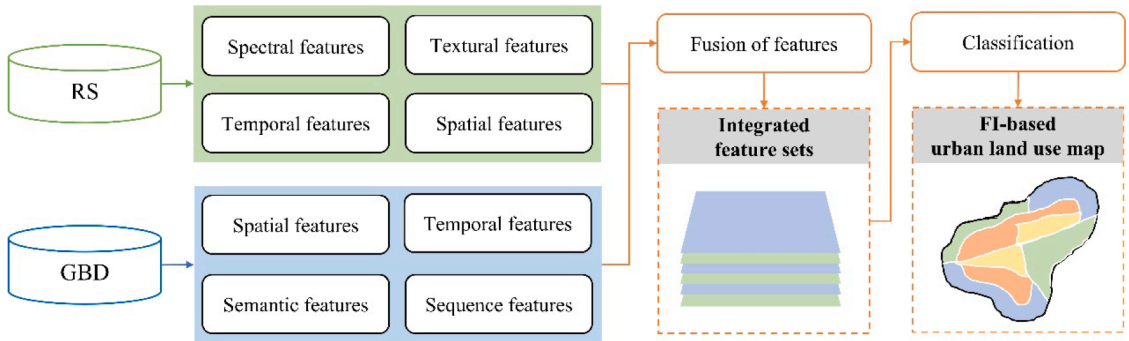

Fig. 3. FI-based categorization strategies.

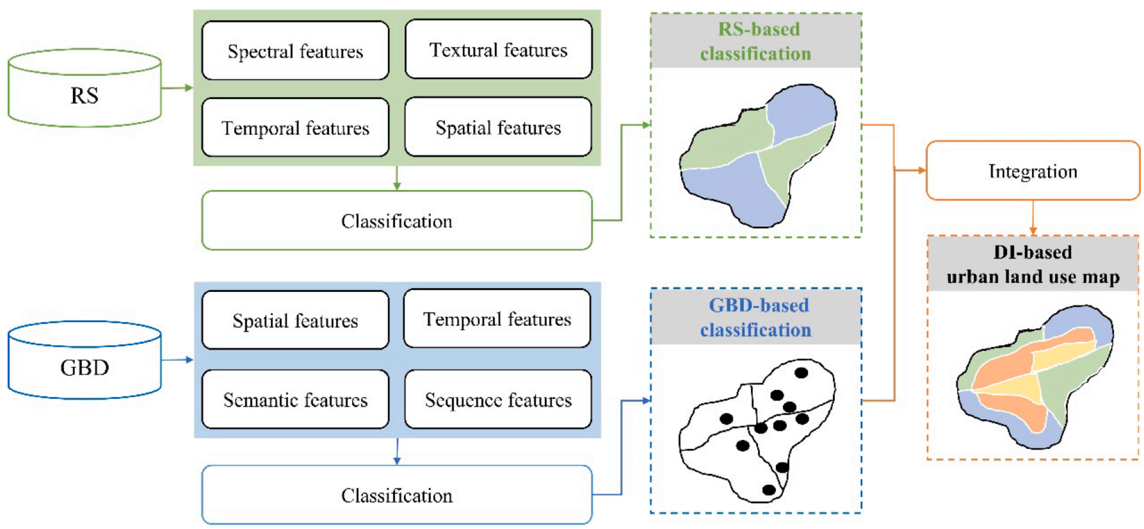

Fig. 4. DI-based categorization strategies.

diverse (Chang et al., 2015). The characteristic of DI-based classification is to combine the RS-based classification and GBD-based classification for extracting urban land use information. It is thus not necessary to unify the spatial units for RS-based classification and GBD-based classification, and the spatial units for the two classification methods will be different. For example, Jia et al. (2018) first classified Gaofen images and mobile phone positioning data by using a support vector machine, and then the two classification results were fused for mapping urban land use based on grid-level units. Tu et al. (2018) utilized the hierarchical cluster analysis to combine RS-based landscape metrics and GBD-based human activity metrics for investigating urban functional patterns in terms of object-based units. In addition, Zhao et al. (2019) delineated the geographical object by using OSM data to train the CNN model. Chen et al. (2018) identified urban green space by utilizing parcels generated by the OSM road networks as the basic units.

There are several methods for the integration of the RS-based classification and GBD-based classification in the DI method based on certain decision fusion strategies such as hierarchical clustering, overlaying, and labeling (Anugraha et al., 2020; Liu et al., 2020b; Xu et al., 2020). For example, Xu et al. (2020) proposed a framework that extracts spatial geographic characteristics from RS images by using deep neural networks and functional distribution characteristics from POIs, and further normalized the two results to identify urban functional regions. Song et al. (2018) used an object-based approach to generate urban objects by using RS data. Then, the objects were further classified and aggregated using POIs. Furthermore, Zhong et al. (2020) presented a method by using the rule-based category mapping (RCM) model to integrate RS-oriented results and GBD-oriented results for extracting urban functional zones. In Zhong's work, POIs data and RS images were classified through different machine learning methods based on the parcel-level unit, then the two results with different classification systems were combined by weighting the word frequency within each parcel.

5. Discussion

5.1. Advantages and disadvantages of FI-based and DI-based classification

The FI method lies in the realization of considerable information compression of RS data and GBD, which is conducive to real-time processing. This method has the advantages of a low level of human intervention and short processing time. In addition, feature optimization and deep interactions between RS and GBD features can be achieved. Several studies have been analyzed to quantify the relative importance of independent features in the FI method (Zhang et al., 2019b). Furthermore, heterogeneity may occur from variations in data quality, time periods, data formats, and data scales, between RS and GBD, resulting in different representations, descriptions, and interpretations of the goal.

The DI-based classification method has been a fundamental contribution of integrating RS and GBD to urban knowledge (Cai et al., 2017; Zhao et al., 2019). RS and GBD features could be calculated and processed respectively in the DI method, which avoids the feature integrating and conflicting issues. Specifically, RS and GBD with various features could be processed by different methods, and then integrated by certain models. However, the accuracies of DI-based classification are affected by the two kinds of processing procedures because the mapping results are obtained by overlapping RS-based classification and GBD-based classification. It is thus important to control the procedures for both RS and GBD classification for high accuracy and better performance.

5.2. Limitations and future consideration for RS and GBD integration

The main limitation is that the modality gap (data structure, data format, and data quality) between RS data and GBD, which brings difficulty for the integration. GBD has different sources (modern sensors, geo-tagged web, ground surveying, mobile mapping, and social media platforms), spatiotemporal resolution, and structures from that of RS data (Ali et al., 2017). For example, the data formats of GBD include the image, geo-tagged text, video, and vector. Comparatively, the most commonly used RS data is a raster (Zhu et al., 2019). Furthermore, GBD is not collected evenly across space because the composition of participation (i.e., sensors, platforms, and social habits) in GBD varies across political, cultural, demographics, and commercial factors, while RS data usually has spatially consistent observation frequencies (Chen et al., 2020; Yu et al., 2018). Some areas might have the data sparsity issue of GBD, which might present problems for mapping based on the integration of RS and GBD owing to the lack of GBD. More specifically, social networking platforms such as WeChat, Sina Weibo, and Tencent are widely used in China, while Twitter, Facebook, and Instagram are more popular in Western countries (Li et al., 2018; Wang et al., 2016; Zhou and Zhang, 2016). The emergence of deep learning technologies provides an opportunity to bridge the gap between different data modalities.

The advances in classification algorithms, computing platforms, and data sources are beneficial for mapping urban land use by integrating RS and GBD. Deep learning, as a novel branch of machine learning, establishes fundamental parameters about the data and trains the computer to learn on its own by detecting patterns using a multi-layered approach (Reichstein et al., 2019; Zhu et al., 2017). Several studies have shown that deep learning is particularly effective in integrating RS and GBD for urban region function recognition (Ma et al., 2019; Qin et al., 2018). Furthermore, the fast growth of cloud computing platforms offers a promising solution for processing large amounts of RS data and GBD. For example, Yin et al. (2021) processed the Sentinel images and POIs data for urban land use classification by using the Google Earth Engine (GEE). GEE could provide a range of data processing methods as well as RS images at various temporal and spatial scales, which is beneficial for improving data computing difficulties (Gorelick et al., 2017). In addition to GEE, other platforms such as Earth Observation Data Center and the Amazon Web Services have also been used for analyzing RS data and GBD on urban land use classification. Furthermore, it is necessary to consider auxiliary data (e.g., census data, statistical data, weather data, hydrological data, and digital elevation data) for more space- and time-referenced information on urban land use classification that integrates RS and GBD (Taubenböck et al., 2009).

5.3. Potential applications of urban land use maps derived from RS and GBD integration

Urban land use maps integrating RS and emerging GBD provide more potential in urban management such as urban planning, urban environment assessment, urban disaster monitoring, and urban traffic analysis (Fig. 5).

A more scientific and efficient urban planning system will benefit from the urban land use map integrating RS and GBD. For example, Xing and Meng (2018) extracted urban land use information by integrating landscape metrics from RS images and semantic features from GBD, which plays as an indicator in urban planning and management. Chen et al. (2018) identified urban green space (e.g., municipal park, community park, etc.) by extracting land cover features from RS data and land use features from POIs for the urban green space planning, which could assist government departments in urban green space planning. In general, integrating RS and GBD would help to improve the city function from the “hard” physical environment and the “soft” services. The addition of GBD for urban land use maps with adequate and timely information could enhance the feedback loops of urban insights for urban governors and panners.

The current advances of urban land use maps that integrate RS data and GBD make it capable of monitoring urban environments such as

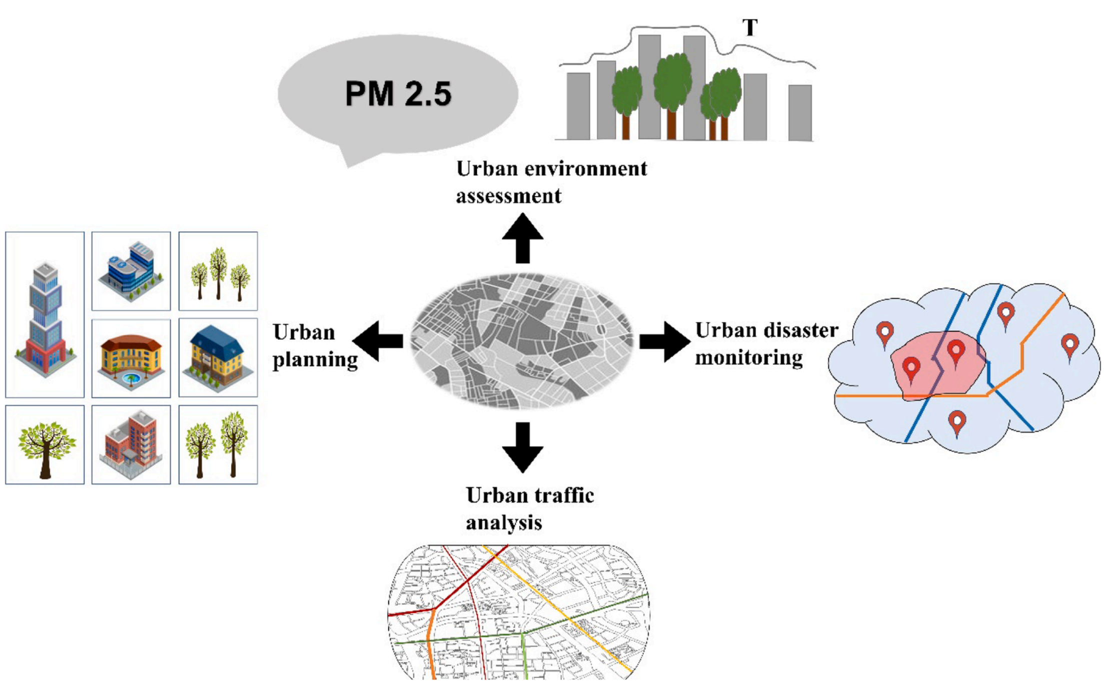

Fig. 5. Urban land use map integrating RS and GBD for urban management.

urban heat island and air pollution (Halim et al., 2020; Masoudi et al., 2021; Venter et al., 2020; Wang et al., 2021). For example, Song et al. (2019) analyzed the relationship between urban functional regions and air pollutant emissions and presented a cost-effective way of mapping spatiotemporal patterns of air pollution by utilizing the urban land use map that integrates RS images and POIs. Luan et al. (2020) quantified the impacts of urban natural surfaces and non-surface human activities on urban heat islands by using RS data and GBD, and explored the relationships between urban heat islands and urban land use patterns. This evidence demonstrated that air pollution concentrations are associated with RS-based urban land cover (e.g., industrial layout) as well as GBD-based urban land use (e.g., travel behavior). Other applications have also proved that the spatial patterns of the urban environments have strong relationships with the urban land use patterns (Pan et al., 2013).

Massive information from urban land use maps that integrate RS and quick-updated GBD is generated continuously and dynamically, providing resources to aid in disaster analysis of historical and future occurrences (earthquakes, fires, or floods) (Huang et al., 2017; Li et al., 2017b). For instance, Li et al. (2019) reviewed recent research that utilized RS and GBD for urban disaster information detection including the suffering area, suffering location, and suffering pattern, which provided a useful method for disaster management. Furthermore, Cervone et al. (2016) proposed a novel framework for urban damage assessment under severe weather by using RS images and real-time Twitter data, which were then combined with other GBD in order to get abundant information in disaster areas. Quickly updated urban land use maps that integrate RS and GBD with fine spatial resolution could support urban disaster management by providing unprecedented reference data.

Up to date, urban traffic conditions have become serious problems that threatening human's daily living quality. Several studies have been made on the comprehensive analysis of urban traffic by taking advantage of RS data and GBD on urban land. Applications in traffic quality analysis, for example, classifying Shanghai city into six traffic "source-sink" areas according to the pick-ups and drop-offs of traffic data and LandScan product (Liu et al., 2012). Improved urban land use maps could also provide technical support for the transportation of the Smart Cities (Zanella et al., 2014). A thorough perception of urban traffic conditions could be achieved through the integration of RS and GBD.

6. Conclusions

This study examined the applications of RS and GBD features in urban land use categorization, as well as methods for RS and GBD integration. The analysis of the existing literature concludes that the emerging GBD provides opportunities for the transformation from urban land cover (physical environment) to urban land use (living environment). Applications on the urban land use maps integrating RS and GBD for urban management mainly include urban planning, urban environment assessment, urban disaster monitoring, and urban traffic analysis. Deeper understandings of the urban surface can be acquired by adding GBD values to the traditional urban RS works. As the integration of RS and GBD has become more generalized, significant progress can be already seen for urban management. Also, integrating RS and GBD on urban land use provides an opportunity for putting people at the center of processes of knowledge and management of the urban planet.

Declaration of Competing Interest

The authors declare that they have no known competing financial interests or personal relationships that could have appeared to influence the work reported in this paper.

Acknowledgements

This study was supported by the Key Research Program of Frontier Sciences (QYZDB-SSW-DQC005) and the Strategic Priority Research Program (XDA19040301) of the Chinese Academy of Sciences (CAS), the National Natural Science Foundation of China (41871349, 41801336, 41971078). Jiadi Yin is supported by a Ph.D. scholarship from the University of Nottingham Ningbo China as part of a doctoral training partnership with the Institute for Geographic Science and Natural Resources Research (IGSNRR), CAS.

Appendix A. Supplementary material

Supplementary data to this article can be found online at https://doi.org/10.1016/j.jag.2021.102514.

References

Ali, A.L., Falomir, Z., Schmid, F., Freksa, C., 2017. Rule-guided human classification of Volunteered Geographic Information. ISPRS J. Photogram. Rem. Sens. 127, 3–15.
Anugraha, A., Chu, H.-J., Ali, M., 2020. Social sensing for urban land use identification. ISPRS Int GEO-INF. 9 (9), 550. https://doi.org/10.3390/ijgi9090550.
Arino, O., Gross, D., Ranera, F., Leroy, M., Bicheron, P., Brockman, C., Defourny, P., Vancutsem, C., Achard, F., Durieux, L., 2007. GlobCover: ESA service for global land cover from MERIS. IGARSS 2007, 2412–2415.
Bao, H., Ming, D., Guo, Y.a., Zhang, K., Zhou, K., Du, S., 2020. DFCNN-based semantic recognition of urban functional zones by integrating remote sensing data and POI data. Remote Sens. 12 (7), 1088. https://doi.org/10.3390/rs12071088.
Bartholomé, E., Belward, A.S., 2005. GLC2000: a new approach to global land cover mapping from Earth observation data. Int. J. Remote Sens. 26 (9), 1959–1977.
Brovelli, M.A., Zamboni, G., Arias Muñoz, C., 2015. From paper maps to the Digital Earth and the Internet of Places. Rendiconti Lincei. 26 (S1), 97–103.
Cadavid Restrepo, A.M., Yang, Y.R., Hamm, N.A.S., Gray, D.J., Barnes, T.S., Williams, G. M., Soares Magalhães, R.J., McManus, D.P., Guo, D., Clements, A.C.A., 2017. Land cover change during a period of extensive landscape restoration in Ningxia Hui Autonomous Region. China. Sci. Total Environ. 598, 669–679.
Cai, J., Huang, B.o., Song, Y., 2017. Using multi-source geospatial big data to identify the structure of polycentric cities. Rem. Sens. Environ. 202, 210–221.
Cao, R., Tu, W., Yang, C., Li, Q., Liu, J., Zhu, J., Zhang, Q., Li, Q., Qiu, G., 2020. Deep learning-based remote and social sensing data fusion for urban region function recognition. ISPRS J. Photogram. Rem. Sens. 163, 82–97.
Cervone, G., Sava, E., Huang, Q., Schnebele, E., Harrison, J., Waters, N., 2016. Using Twitter for tasking remote-sensing data collection and damage assessment: 2013 Boulder flood case study. Int. J. Remote Sens. 37 (1), 100–124.
Chang, C., Ye, Z., Huang, Q., Wang, C., 2015. An integrative method for mapping urban land use change using "geo-sensor" data. In: UrbanGIS'15: Proceedings of the 1st International ACM SIGSPATIAL Workshop on Smart Cities and Urban Analytics, pp. 47–54.
Chang, S., Wang, Z., Mao, D., Guan, K., Jia, M., Chen, C., 2020. Mapping the essential urban land use in Changchun by applying random forest and multi-Source geospatial data. Remote Sens. 12 (15), 2488. https://doi.org/10.3390/rs12152488.
Chen, B., Song, Y., Huang, B.o., Xu, B., 2020. A novel method to extract urban human settlements by integrating remote sensing and mobile phone locations. Science of Remote Sensing. 1, 100003. https://doi.org/10.1016/j.srs.2020.100003.
Chen, J., Chen, J., Liao, A., Cao, X., Chen, L., Chen, X., He, C., Han, G., Peng, S., Lu, M., Zhang, W., Tong, X., Mills, J., 2015. Global land cover mapping at 30m resolution: A POK-based operational approach. ISPRS J. Photogram. Rem. Sens. 103, 7–27.
Chen, W., Huang, H., Dong, J., Zhang, Y., Tian, Y., Yang, Z., 2018. Social functional mapping of urban green space using remote sensing and social sensing data. ISPRS J. Photogram. Rem. Sens. 146, 436–452.
Chen, Y., Liu, X., Li, X., Liu, X., Yao, Y., Hu, G., Xu, X., Pei, F., 2017. Delineating urban functional areas with building-level social media data: A dynamic time warping (DTW) distance based k-medoids method. Landsc Urban Plan. 160, 48–60.
CIESIN, IFPRI, CIAT, 2011. Global Rural-Urban Mapping Project, Version 1 (GRUMPv1): Land and Geographic Unit Area Grids. Palisades, NY: NASA Socioeconomic Data and Applications Center (SEDAC).
Colstoun, B.d., C, E., Huang, C., Wang, P., Tilton, J.C., Tan, B., Phillips, J., Niemczura, S., Ling, P.Y., Wolfe, R.E., 2017. Global Man-made Impervious Surface (GMIS) Dataset From Landsat. Palisades, NY: NASA Socioeconomic Data and Applications Center (SEDAC).
Defourny, P., Kirches, G., Brockmann, C., Boettcher, M., Peters, M., Bontemps, S., Lamarche, C., Schlerf, M., M., S., 2018. Land Cover CCI: Product User Guide Version 2.
Deng, Jinsong, Huang, Yibo, Chen, Binjie, Tong, Cheng, Liu, Pengbo, Wang, Hongquan, Hong, Yang, 2019. A methodology to monitor urban expansion and green space change using a time series of multi-sensor SPOT and Sentinel-2A images. Remote Sens. 11 (10), 1230. https://doi.org/10.3390/rs11101230.
Dong, J., Xiao, X., 2016. Evolution of regional to global paddy rice mapping methods: A review. ISPRS J. Photogram. Rem. Sens. 119, 214–227.
Dong, X., Xu, Y., Huang, L., Liu, Z., Xu, Y., Zhang, K., Hu, Z., Wu, G., 2020. Exploring impact of spatial unit on urban land use mapping with multisource data. Remote Sens. 12.
Du, S.J., Du, S.H., Liu, B., Zhang, X.Y., Zheng, Z.J., 2020. Large-scale urban functional zone mapping by integrating remote sensing images and open social data. GIsci Remote Sens. 57, 411–430.

Ellis, E.C., Ramankutty, N., 2008. Putting people in the map: anthropogenic biomes of the world. Front Ecol Environ. 6, 439–447.
Elmqvist, T., Andersson, E., Frantzeskaki, N., McPhearson, T., Olsson, P., Gaffney, O., Takeuchi, K., Folke, C., 2019. Sustainability and resilience for transformation in the urban century. Nat. Sustain. 2, 267–273.
Elvidge, C.D., Tuttle, B.T., Sutton, P.C., Baugh, K.E., Howard, A.T., Milesi, C., Bhaduri, B. L., Nemani, R., 2007. Global distribution and density of constructed impervious surfaces. Sensors. 1962–1979.
Esch, T., Taubenboeck, H., Roth, A., Heldens, W., Felbier, A., Thiel, M., Schmidt, M., Mueller, A., Dech, S., 2012. TanDEM-X mission-new perspectives for the inventory and monitoring of global settlement patterns. J. Appl. Remote, Sens, p. 6.
Frias-Martinez, V., Frias-Martinez, E., 2014. Spectral clustering for sensing urban land use using Twitter activity. Eng Appl Artif Intell. 35, 237–245.
Friedl, M.A., McIver, D.K., Hodges, J.C.F., Zhang, X.Y., Muchoney, D., Strahler, A.H., Woodcock, C.E., Gopal, S., Schneider, A., Cooper, A., Baccini, A., Gao, F., Schaaf, C., 2002. Global land cover mapping from MODIS: algorithms and early results. Rem. Sens. Environ. 83, 287–302.
Gong, L., Liu, X., Wu, L., Liu, Y., 2015. Inferring trip purposes and uncovering travel patterns from taxi trajectory data. Cartogr Geogr Inf Sci. 43, 103–114.
Gong, P., Chen, B., Li, X., Liu, H., Wang, J., Bai, Y., Chen, J., Chen, X., Fang, L., Feng, S., Feng, Y., Gong, Y., Gu, H., Huang, H., Huang, X., Jiao, H., Kang, Y., Lei, G., Li, A., Li, X., Li, X., Li, Y., Li, Z., Li, Z., Liu, C., Liu, C., Liu, M., Liu, S., Mao, W., Miao, C., Ni, H., Pan, Q., Qi, S., Ren, Z., Shan, Z., Shen, S., Shi, M., Song, Y., Su, M., Suen, H.P., Sun, B., Sun, F., Sun, J., Sun, L., Sun, W., Tian, T., Tong, X., Tseng, Y., Tu, Y., Wang, H., Wang, L., Wang, X., Wang, Z., Wu, T., Xie, Y., Yang, J., Yang, J., Yuan, M., Yue, W., Zeng, H., Zhang, K., Zhang, N., Zhang, T., Zhang, Y., Zhao, F., Zheng, Y., Zhou, Q., Clinton, N., Zhu, Z., Xu, B., 2020. Mapping essential urban land use categories in China (EULUC-China): preliminary results for 2018. Sci. Bull. 65, 182–187.
Gong, P., Howarth, P.J., 1989. Performance analyses of probabilistic relaxation methods for land-cover classification. Rem. Sens. Environ. 30, 33–42.
Gong, P., Li, X., Zhang, W., 2019a. 40-Year (1978–2017) human settlement changes in China reflected by impervious surfaces from satellite remote sensing. Sci. Bull. 64, 756–763.
Gong, P., Liu, H., Zhang, M., Li, C., Wang, J., Huang, H., Clinton, N., Ji, L., Li, W., Bai, Y., Chen, B., Xu, B., Zhu, Z., Yuan, C., Ping Suen, H., Guo, J., Xu, N., Li, W., Zhao, Y., Yang, J., Yu, C., Wang, X., Fu, H., Yu, L., Dronova, I., Hui, F., Cheng, X., Shi, X., Xiao, F., Liu, Q., Song, L., 2019b. Stable classification with limited sample: transferring a 30-m resolution sample set collected in 2015 to mapping 10-m resolution global land cover in 2017. Sci. Bull. 64, 370–373.
Gong, P., Wang, J., Yu, L., Zhao, Y., Zhao, Y., 2013. Finer resolution observation and monitoring of global land cover: first mapping results with Landsat TM and ETM+ data. Int. J. Remote Sens. 34, 2607–2654.
Goodchild, M.F., Glennon, J.A., 2010. Crowdsourcing geographic information for disaster response: a research frontier. Int J Digit Earth. 3, 231–241.
Gorelick, N., Hancher, M., Dixon, M., Ilyushchenko, S., Thau, D., Moore, R., 2017. Google Earth Engine: Planetary-scale geospatial analysis for everyone. Rem. Sens. Environ. 202, 18–27.
Halim, N.D.A., Latif, M.T., Mohamed, A.F., Maulud, K.N.A., Idrus, S., Azhari, A., Othman, M., Sofwan, N.M., 2020. Spatial assessment of land use impact on air quality in mega urban regions. Malaysia. Sustain. Cities Soc. 63, 102436.
Hansen, M.C., Defries, R.S., Townshend, J.R.G., Sohlberg, R., 2000. Global land cover classification at 1km spatial resolution using a classification tree approach. Int. J. Remote Sens. 21, 1331–1364.
Haralick, R.M., Shanmugam, K., Dinstein, I.h., 1973. Textural features for image classification. Studies in Media and Communication. 3, 610-621.
Heiden, U., Segl, K., Roessner, S., Kaufmann, H., 2007. Determination of robust spectral features for identification of urban surface materials in hyperspectral remote sensing data. Rem. Sens. Environ. 111, 537–552.
Helbich, M., Amelunxen, C., Neis, P., Zipf, A., 2012. In: Comparative spatial analysis of positional accuracy of OpenStreetMap and proprietary Geodata. Society and Learning, Salzburg, Germany, pp. 4–6.
Herold, M., Gardner, M.E., Roberts, D.A., 2003. Spectral resolution requirements for mapping urban areas. IEEE Trans Geosci Remote Sens. 41, 1907–1919.
Hersperger, A.M., Oliveira, E., Pagliarin, S., Palka, G., Verburg, P., Bolliger, J., Grădinaru, S., 2018. Urban land-use change: The role of strategic spatial planning. Glob Environ Change. 51, 32–42.
Howarth, P.J., Boasson, E., 1983. Landsat digital enhancements for change detection in urban environments. Rem. Sens. Environ. 13, 149–160.
Hu, T., Yang, J., Li, X., Gong, P., 2016. Mapping urban land use by using Landsat images and open social data. Remote Sens. 8, 151.
Hu, Y., Gao, S., Janowicz, K., Yu, B., Li, W., Prasad, S., 2015. Extracting and understanding urban areas of interest using geotagged photos. Comput Environ Urban Syst. 54, 240–254.
Huang, Q., Cervone, G., Zhang, G., 2017. A cloud-enabled automatic disaster analysis system of multi-sourced data streams: An example synthesizing social media, remote sensing and Wikipedia data. Comput Environ Urban Syst. 66, 23–37.
Huang, R., Taubenbock, H., Mou, L., Zhu, X., 2018. Classificaiton of settlement types from Tweets using LDA and LSTM. IGARSS 2018, 6408–6411.
Huang, Z., Qi, H., Kang, C., Su, Y., Liu, Y., 2020. An ensemble learning approach for urban land use mapping based on remote sensing imagery and social sensing data. Remote Sens. 12.
Huang, X., Haung, J., Wen, D., Li, J., 2021. An updated MODIS global urban extent product (MGUP) from 2001 to 2018 based on an automated mapping approach. Int J Appl Earth Obs Geoinf. 95.
Ilieva, R.T., McPhearson, T., 2018. Social-media data for urban sustainability. Nat. Sustain. 1, 553–565.
Jia, Y., Ge, Y., Ling, F., Guo, X., Wang, J., Wang, L., Chen, Y., Li, X., 2018. Urban land use mapping by combining remote sensing imagery and mobile phone positioning data. Remote Sens. 10.
Jiang, Q., Kresin, F., Arnold K. Bregt, Kooistra, L., Pareschi, E., Putten, E.v., Volten, H., Wesseling, J., 2016. Citizen sensing for improved urban environmental monitoring. J. Sensors. 1-9.
Jin, H., Mountrakis, G., Stehman, S.V., 2014. Assessing integration of intensity, polarimetric scattering, interferometric coherence and spatial texture metrics in PALSAR-derived land cover classification. ISPRS J. Photogram. Rem. Sens. 98, 70–84.
Johnson, B.A., Iizuka, K., 2016. Integrating OpenStreetMap crowdsourced data and Landsat time-series imagery for rapid land use/land cover (LULC) mapping: Case study of the Laguna de Bay area of the Philippines. Appl Geogr. 67, 140–149.
Kang, J., Körner, M., Wang, Y., Taubenböck, H., Zhu, X.X., 2018. Building instance classification using street view images. ISPRS J. Photogram. Rem. Sens. 145, 44–59.
Kitchin, R., 2013. Big data and human geography. Dialogues in Human Geography. 3, 262–267.
Kitchin, R., McArdle, G., 2016. What makes Big Data, Big Data? Exploring the ontological characteristics of 26 datasets. Big Data & Society. 3.
Krylov, V., Kenny, E., Dahyot, R., 2018. Automatic discovery and geotagging of objects from street view imagery. Remote Sens. 10, 661.
Kuffer, M., Pfeffer, K., Sliuzas, R., 2016. Slums from space-15 years of slum mapping using remote sensing. Remote Sens. 8.
Li, J., Benediktsson, J.A., Zhang, B., Yang, T., Plaza, A., 2017a. Spatial technology and social media in remote sensing: challenges and opportunities. P IEEE. 105, 1583–1585.
Li, J., He, Z., Plaza, J., Li, S., Chen, J., Wu, H., Wang, Y., Liu, Y., 2017b. Social media: New perspectives to improve remote sensing for emergency response. P IEEE. 105, 1900–1912.
Li, J., Ying, L., Dang, A., 2018. Live-Work-Play Centers of Chinese cities: Identification and temporal evolution with emerging data. Comput Environ Urban Syst. 71, 58–66.
Li, S., Dragicevic, S., Castro, F.A., Sester, M., Winter, S., Coltekin, A., Pettit, C., Jiang, B., Haworth, J., Stein, A., Cheng, T., 2016. Geospatial big data handling theory and methods: A review and research challenges. ISPRS J. Photogram. Rem. Sens. 115, 119–133.
Li, W., Dong, R., Fu, H., Wang, J., Yu, L., Gong, P., 2020a. Integrating Google Earth imagery with Landsat data to improve 30-m resolution land cover mapping. Rem. Sens. Environ. 237, 111563.
Li, X., Hu, T., Gong, P., Du, S., Chen, B., Li, X., Dai, Q., 2021. Mapping Essential Urban Land Use Categories in Beijing with a Fast Area of Interest (AOI)-Based Method. Remote Sens. 13.
Li, X., Zhou, Y., Zhu, Z., Cao, W., 2020b. A national dataset of 30 m annual urban extent dynamics (1985–2015) in the conterminous United States. Earth Syst. Sci. Data. 12, 357–371.
Li, Z., Huang, Q., Emrich, C.T., 2019. Introduction to social sensing and big data computing for disaster management. Int J Digit Earth. 12, 1198–1204.
Liu, D., Chen, N., Zhang, X., Wang, C., Du, W., 2020a. Annual large-scale urban land mapping based on Landsat time series in Google Earth Engine and OpenStreetMap data: A case study in the middle Yangtze River basin. ISPRS J. Photogram. Rem. Sens. 159, 337–351.
Liu, H., Xu, Y., Tang, J., Deng, M., Huang, J., Yang, W., Wu, F., 2020b. Recognizing urban functional zones by a hierarchical fusion method considering landscape features and human activities. Trans GIS. 24, 1359–1381.
Liu, J., Li, J., Li, W., Wu, J., 2016. Rethinking big data: A review on the data quality and usage issues. ISPRS J. Photogram. Rem. Sens. 115, 134–142.
Liu, X., He, J., Yao, Y., Zhang, J., Liang, H., Wang, H., Hong, Y., 2017. Classifying urban land use by integrating remote sensing and social media data. Int J Geogr Inf Sci. 31, 1675–1696.
Liu, X., Hu, G., Chen, Y., Li, X., Xu, X., Li, S., Pei, F., Wang, S., 2018. High-resolution multi-temporal mapping of global urban land using Landsat images based on the Google Earth Engine Platform. Rem. Sens. Environ. 209, 227–239.
Liu, Y., Liu, X., Gao, S., Gong, L., Kang, C., Zhi, Y., Chi, G., Shi, L., 2015. Social sensing: A new approach to understanding our socioeconomic environments. Ann Assoc Am Geogr. 105, 512–530.
Liu, Y., Wang, F., Xiao, Y., Gao, S., 2012. Urban land uses and traffic 'source-sink areas': Evidence from GPS-enabled taxi data in Shanghai. Landsc Urban Plan. 106, 73–87.
Long, Y., Liu, L., 2017. How green are the streets? An analysis for central areas of Chinese cities using Tencent Street View. PLoS One. 12.
Long, Y., Zhai, W., Shen, Y., Ye, X., 2018. Understanding uneven urban expansion with natural cities using open data. Landsc Urban Plan. 177, 281–293.
Loveland, T.R., Reed, B.C., Brown, J.F., Ohlen, D.O., Zhu, Z., Yang, L., Merchant, J.W., 2000. Development of a global land cover characteristics database and IGBP DISCover from 1 km AVHRR data. Int. J. Remote Sens. 21, 1303–1330.
Lu, D., Weng, Q., 2006. Use of impervious surface in urban land-use classification. Rem. Sens. Environ. 102, 146–160.
Luan, X.L., Yu, Z.W., Zhang, Y.T., Wei, S., Miao, X.Y., Huang, Z.Y.X., Teng, S.Q.N., Xu, C., 2020. Remote sensing and social sensing data reveal scale-dependent and system-specific strengths of urban heat island determinants. Remote Sens. 12.
Ma, L., Liu, Y., Zhang, X., Ye, Y., Yin, G., Johnson, B.A., 2019. Deep learning in remote sensing applications: A meta-analysis and review. ISPRS J. Photogram. Rem. Sens. 152, 166–177.
Mao, W., Lu, D., Hou, L., Liu, X., Yue, W., 2020. Comparison of machine-learning methods for urban land-use mapping in Hangzhou City. China, Remote Sens, p. 12.

Martí, P., Serrano-Estrada, L., Nolasco-Cirugeda, A., 2019. Social Media data: Challenges, opportunities and limitations in urban studies. Comput Environ Urban Syst. 74, 161–174.
Masoudi, M., Tan, P.Y., Fadaei, M., 2021. The effects of land use on spatial pattern of urban green spaces and their cooling ability. Urban Clim. 35, 100743.
Mitchell, L., Frank, M.R., Harris, K.D., Dodds, P.S., Danforth, C.M., 2013. The geography of happiness: connecting twitter sentiment and expression, demographics, and objective characteristics of place. PLoS One. 8, 1–15.
Okujeni, A., Canters, F., Cooper, S.D., Degerickx, J., Heiden, U., Hostert, P., Priem, F., Roberts, D.A., Somers, B., van der Linden, S., 2018. Generalizing machine learning regression models using multi-site spectral libraries for mapping vegetation-impervious-soil fractions across multiple cities. Rem. Sens. Environ. 216, 482–496.
Pacifici, F., Chini, M., Emery, W.J., 2009. A neural network approach using multi-scale textural metrics from very high-resolution panchromatic imagery for urban land-use classification. Rem. Sens. Environ. 113, 1276–1292.
Pan, G., Qi, G., Wu, Z., Zhang, D., Li, S., 2013. Land-Use Classification Using Taxi GPS Traces. IEEE Trans. Intell. Transp. Syst. 14, 113–123.
Patino, J.E., Duque, J.C., 2013. A review of regional science applications of satellite remote sensing in urban settings. Comput Environ Urban Syst. 37, 1–17.
Pei, T., Sobolevsky, S., Ratti, C., Shaw, S.-L., Li, T., Zhou, C., 2014. A new insight into land use classification based on aggregated mobile phone data. Int J Geogr Inf Sci. 28, 1988–2007.
Pesaresi, M., Guo, H., Blaes, X., Ehrlich, D., Ferri, S., Gueguen, L., Halkia, M., Kauffmann, M., Kemper, T., Lu, L., Marin-Herrera, M.A., Ouzounis, G.K., Scavazzon, M., Soille, P., Syrris, V., Zanchetta, L., 2013. A global human settlement layer from optical HR/VHR RS data: Concept and first results. IEEE J. Sel. Topics Appl. Earth Observ. Remote Sens. 6, 2102–2131.
Pflugmacher, D., Rabe, A., Peters, M., Hostert, P., 2019. Mapping pan-European land cover using Landsat spectral-temporal metrics and the European LUCAS survey. Remote Sens Environ. 221, 583–595.
Qi, L., Li, J., Wang, Y., Gao, X., 2019. Urban Observation: Integration of remote sensing and social media data. IEEE J. Sel. Topics Appl. Earth Observ. Remote Sens. 1–13.
Qin, Y., Chi, M., Liu, X., Zhang, Y., Zeng, Y., Zhao, Z., 2018. Classification of high resolution urban remote sensing images using deep networks by integration of social media photos. IGARSS 2018, 7243–7246.
Reba, M., Seto, K.C., 2020. A systematic review and assessment of algorithms to detect, characterize, and monitor urban land change. Rem. Sens. Environ. 242, 111739.
Reichstein, M., Camps-Valls, G., Stevens, B., Jung, M., Denzler, J., Carvalhais, N., Prabhat, 2019. Deep learning and process understanding for data-driven Earth system science. Nature. 566, 195-204.
Schneider, A., Friedl, M.A., Potere, D., 2010. Mapping global urban areas using MODIS 500-m data: New methods and datasets based on 'urban ecoregions'. Remote Sens Environ. 114, 1733–1746.
Seto, K.C., Fragkias, M., Guneralp, B., Reilly, M.K., 2011. A meta-analysis of global urban land expansion. PLoS One. 6.
Shi, Y., Qi, Z., Liu, X., Niu, N., Zhang, H., 2019. Urban land use and land cover classification using multisource remote sensing images and social media data. Remote Sens. 11, 2719.
Song, J., Lin, T., Li, X., Prishchepov, A.V., 2018. Mapping urban functional zones by integrating very high spatial resolution remote sensing imagery and points of interest: A case study of Xiamen. China. Remote Sens. 10, 1737.
Song, J., Zhao, C., Lin, T., Li, X., Prishchepov, A.V., 2019. Spatio-temporal patterns of traffic-related air pollutant emissions in different urban functional zones estimated by real-time video and deep learning technique. J. Clean. Prod. 238, 117881.
Song, X., Feng, Q., Xia, F., Li, X., Scheffran, J., 2021. Impacts of changing urban land-use structure on sustainable city growth in China: A population-density dynamics perspective. Habitat Int. 107, 102296.
Srivastava, S., Vargas Muñoz, J.E., Lobry, S., Tuia, D., 2018. Fine-grained landuse characterization using ground-based pictures: a deep learning solution based on globally available data. Int J Geogr Inf Sci. 1–20.
Steffen, W., Grinevald, J., Crutzen, P., McNeill, J., 2011. The Anthropocene: conceptual and historical perspectives. Philosophical Transactions of the Royal Society A: Mathematical, Physical and Engineering Sciences. 369, 842–867.
Sun, J., Wang, H., Song, Z., Lu, J., Meng, P., Qin, S., 2020. Mapping essential urban land use categories in Nanjing by integrating multi-source Big Data. Remote Sens. 12.
Taubenböck, H., Wurm, M., Setiadi, N., Gebert, N., Roth, A., Strunz, G., Birkmann, J., Dech, S., 2009. Integrating remote sensing and social science-The correlation of urban morphology with socioeconomic parameters. Joint Urban Remote Sensing Event. 2009, 1–7.
Tu, W., Hu, Z., Li, L., Cao, J., Jiang, J., Li, Q., Li, Q., 2018. Portraying urban functional zones by coupling remote sensing imagery and human sensing data. Remote Sens. 10.
Ursula, C., Benz, and, Peter, Hofmann, and, Gregor, Willhauck, and, 2004. Multi-resolution, object-oriented fuzzy analysis of remote sensing data for GIS-ready information. ISPRS J. Photogram. Rem. Sens. 58, 239-258.
Venter, Z.S., Brousse, O., Esau, I., Meier, F., 2020. Hyperlocal mapping of urban air temperature using remote sensing and crowdsourced weather data. Rem. Sens, Environ, p. 242.
Wan, T., Lu, H., Lu, Q., Luo, N., 2017. Classification of high-resolution remote-sensing image using OpenStreetMap information. IEEE Geosci. Remote. Sens. Lett. 14, 2305–2309.
Wang, G., Han, Q., de vries, B., 2021. The multi-objective spatial optimization of urban land use based on low-carbon city planning. Ecol Indic 125, 107540.
Wang, P., Huang, C., Brown de Colstoun, E.C., Tilton, J.C., Tan, B., 2017. Global human built-up and settlement extent (HBASE) dataset from Landsat. NASA Socioeconomic Data and Applications Center (SEDAC), Palisades, NY.
Wang, Y., Wang, T., Tsou, M.-H., Li, H., Jiang, W., Guo, F., 2016. Mapping dynamic urban land use patterns with crowdsourced geo-tagged social media (Sina-Weibo) and commercial Points of interest collections in Beijing. China. Sustainability. 8, 1202.
Weng, Q., Hu, X., Liu, H., 2009. Estimating impervious surfaces using linear spectral mixture analysis with multitemporal ASTER images. Int. J. Remote Sens. 30, 4807–4830.
Wu, H., Zhang, T., Gong, J., 2015. GeoComputation for geospatial big data. Trans GIS 18, 1–2.
Wu, L., Cheng, X., Kang, C., Zhu, D., Huang, Z., Liu, Y., 2018. A framework for mixed-use decomposition based on temporal activity signatures extracted from big geo-data. Int J Digit Earth. 1–19.
Wurm, M., Taubenböck, H., Weigand, M., Schmitt, A., 2017. Slum mapping in polarimetric SAR data using spatial features. Rem. Sens. Environ. 194, 190–204.
Xing, H., Meng, Y., 2018. Integrating landscape metrics and socioeconomic features for urban functional region classification. Comput Environ Urban Syst. 72, 134–145.
Xiong, G., Cao, X., Hamm, N.A.S., Lin, T., Zhang, G., Chen, B., 2021. Unbalanced Development Characteristics and Driving Mechanisms of Regional Urban Spatial Form: A Case Study of Jiangsu Province. China, Sustainability, p. 13.
Xu, G., Zhu, X., Fu, D., Dong, J., Xiao, X., 2017. Automatic land cover classification of geo-tagged field photos by deep learning. Environ Model Softw. 91, 127–134.
Xu, S., Qing, L., Han, L., Liu, M., Peng, Y., Shen, L., 2020. A new remote sensing images and point-of-interest fused (RPF) model for sensing urban functional regions. Remote Sens. 12.
Yammine, S.Z., Jarreau, P.B., Liu, C., Coe, I.R., 2018. Social media for social change in science. Science. 360, 163.
Yang, W., Mu, L., 2015. GIS analysis of depression among Twitter users. Appl Geogr. 60, 217–223.
Yao, Y., Zhang, J., Hong, Y., Liang, H., He, J., 2018. Mapping fine-scale urban housing prices by fusing remotely sensed imagery and social media data. Trans GIS. 22, 561–581.
Ye, X., Huang, Q., Li, W., 2016. Integrating big social data, computing and modeling for spatial social science. Cartogr Geogr Inf Sci. 43, 377–378.
Yin, J., Fu, P., Hamm, N.A.S., Li, Z., You, N., He, Y., Cheshmehzangi, A., Dong, J., 2021. Decision-level and feature-level integration of remote sensing and geospatial big data for urban land use mapping. Remote Sens. 13.
Yu, B., Lian, T., Huang, Y., Yao, S., Ye, X., Chen, Z., Yang, C., Wu, J., 2019. Integration of nighttime light remote sensing images and taxi GPS tracking data for population surface enhancement. Int J Geogr Inf Sci. 33, 687–706.
Yu, Y., Li, J., Zhu, C., Plaza, A., 2018. Urban impervious surface estimation from remote sensing and social data. Photogramm Eng Remote Sensing. 84, 771–780.
Zanella, A., Bui, N., Castellani, A., Vangelista, L., Zorzi, M., 2014. Internet of Things for Smart Cities. IEEE Internet Things J. 1, 22–32.
Zhan, X., Ukkusuri, S.V., Zhu, F., 2014. Inferring urban land use using large-scale social media check-in data. Netw. Spat. Econ. 14, 647–667.
Zhang, C., Xu, L., Yan, Z., Wu, S., 2021a. A GloVe-Based POI Type Embedding Model for Extracting and Identifying Urban Functional Regions. ISPRS Int. J, Geoinf, p. 10.
Zhang, F., Wu, L., Zhu, D., Liu, Y., 2019a. Social sensing from street-level imagery: A case study in learning spatio-temporal urban mobility patterns. ISPRS J. Photogram. Rem. Sens. 153, 48–58.
Zhang, J., Li, X., Yao, Y., Hong, Y., He, J., Jiang, Z., Sun, J., 2021b. The Traj2Vec model to quantify residents' spatial trajectories and estimate the proportions of urban land-use types. Int J Geogr Inf Sci. 35, 193–211.
Zhang, X., Du, S., Wang, Q., 2017a. Hierarchical semantic cognition for urban functional zones with VHR satellite images and POI data. ISPRS J. Photogram. Rem. Sens. 132, 170–184.
Zhang, X., Du, S., Zheng, Z., 2020. Heuristic sample learning for complex urban scenes: Application to urban functional-zone mapping with VHR images and POI data. ISPRS J. Photogram. Rem. Sens. 161, 1–12.
Zhang, Y., Li, Q., Huang, H., Wu, W., Du, X., Wang, H., 2017b. The combined use of remote sensing and social sensing data in fine-grained urban land use mapping: A case study in Beijing. China. Remote Sens. 9, 865.
Zhang, Y., Li, Q., Tu, W., Mai, K., Yao, Y., Chen, Y., 2019b. Functional urban land use recognition integrating multi-source geospatial data and cross-correlations. Comput Environ Urban Syst. 78, 101374.
Zhao, N., Cao, G., Zhang, W., Samson, E.L., 2018. Tweets or nighttime lights: Comparison for preeminence in estimating socioeconomic factors. ISPRS J. Photogram. Rem. Sens. 146, 1–10.
Zhao, W., Bo, Y., Chen, J., Tiede, D., Blaschke, T., Emery, W.J., 2019. Exploring semantic elements for urban scene recognition: Deep integration of high-resolution imagery and OpenStreetMap (OSM). ISPRS J. Photogram. Rem. Sens. 151, 237–250.
Zheng, S., Wang, J., Sun, C., Zhang, X., Kahn, M.E., 2019. Air pollution lowers Chinese urbanites' expressed happiness on social media. Nat. Hum. Behav. 3, 237–243.
Zhong, Y., Su, Y., Wu, S., Zheng, Z., Zhao, J., Ma, A., Zhu, Q., Ye, R., Li, X., Pellikka, P., Zhang, L., 2020. Open-source data-driven urban land-use mapping integrating point-line-polygon semantic objects: A case study of Chinese cities. Rem. Sens, Environ, p. 247.
Zhou, X., Zhang, L., 2016. Crowdsourcing functions of the living city from Twitter and Foursquare data. Cartogr Geogr Inf Sci. 43, 393–404.
Zhou, Y., Li, X., Asrar, G.R., Smith, S.J., Imhoff, M., 2018. A global record of annual urban dynamics (1992–2013) from nighttime lights. Rem. Sens. Environ. 219, 206–220.
Zhu, X., Tuia, D., Mou, L., Xia, G., Zhang, L., Xu, F., Fraundorfer, F., 2017. Deep learning in remote sensing: A comprehensive review and list of resources. IEEE Geosci. Remote Sens. Mag. 5, 8–36.

Zhu, Z., Woodcock, C.E., Rogan, J., Kellndorfer, J., 2012. Assessment of spectral, polarimetric, temporal, and spatial dimensions for urban and peri-urban land cover classification using Landsat and SAR data. Rem. Sens. Environ. 117, 72–82.

Zhu, Z., Zhou, Y., Seto, K.C., Stokes, E.C., Deng, C., Pickett, S.T.A., Taubenböck, H., 2019. Understanding an urbanizing planet: Strategic directions for remote sensing. Rem. Sens. Environ. 228, 164–182.

Zurita-Milla, R., Gijsel, J.A.E.v., Hamm, N.A.S., Augustijn, P.W.M., Vrieling, A., 2013. Exploring Spatiotemporal Phenological Patterns and Trajectories Using Self-Organizing Maps. IEEE Trans Geosci Remote Sens. 51, 1914-1921.